The Journal of Nutrition 153 (2023) 3448–3457

American Society for Nutrition
Excellence in Nutrition Research and Practice

JN THE JOURNAL OF NUTRITION

journal homepage: https://jn.nutrition.org/

Nutrient Physiology, Metabolism, and Nutrient-Nutrient Interactions

Dietary Galactose Increases the Expression of Mitochondrial OXPHOS Genes and Modulates the Carbohydrate Oxidation Pathways in Mouse Intestinal Mucosa

Ferran S. Fos-Codoner, Lianne M.S. Bouwman, Jaap Keijer, Evert M. van Schothorst *

Human and Animal Physiology, Wageningen University, Wageningen, The Netherlands

A B S T R A C T

Background: Prolonged lactation provides substantial health benefits, possibly because of galactose as part of milk sugar lactose. Isocaloric replacement of dietary glucose [16 energy%(en%)] with galactose within a normal diet (64en% carbohydrates) during a 3-wk postweaning period provided substantial benefits on short- and long-term physiologic and metabolic parameters at the whole-body level and liver in female mice, which might be attributable to intestinal function.

Objectives: This study aimed to investigate if partial dietary replacement of glucose with galactose alters intestinal metabolism underlying hepatic health effects.

Methods: Proximal intestinal mucosa gene profiles in female mice were analyzed using RNAseq technology, validated, and correlated with hepatic health parameters.

Results: Transcriptome analysis revealed that the presence of galactose primarily affected the pathways involved in energy metabolism. A consistently higher expression was observed in the subset of mitochondrial transcripts (78 of 80, all *P*.adj < 0.1). Oxidative phosphorylation (OXPHOS) represented the most upregulated process (all top 10 pathways) independent of the total mitochondrial mass ($P = 0.75$). Moreover, galactose consistently upregulated carbohydrate metabolism pathways, specifically glycolysis till acetyl-CoA production and fructose metabolism. Also, the expression of transcripts involved in these pathways was negatively correlated with circulating serum amyloid A3 protein, a marker of hepatic inflammation [R (−0.61, −0.5), *P* (0.002, 0.01)]. Accordingly, $CD163^+$ cells were decreased in the liver. Additionally, the expression of key fructolytic enzymes in the small intestinal mucosa was negatively correlated with triglyceride accumulation in the liver [R (−0.45, −0.4), *P* (0.03, 0.05)].

Conclusions: To our knowledge, our results show for the first time the role of galactose as an OXPHOS activator in vivo. Moreover, the concept of intestinal cells acting as the body's metabolic gatekeeper is strongly supported, as they alter substrate availability and thereby contribute to the maintenance of metabolic homeostasis, protecting other organs, as evidenced by their potential ability to shield the liver from the potentially detrimental effects of fructose.

Keywords: mouse, galactose, lactose, OXPHOS, gut-liver axis, carbohydrate metabolism, mitochondria, RNAseq

Introduction

The milk sugar lactose is a glucose–galactose disaccharide found almost exclusively in mammalian milk and represents the most abundant molecule of its carbohydrate fraction [1]. Glucose is ubiquitously present in our diet, whereas galactose is mainly taken in as part of the lactose molecule [1]. After lactose is consumed, it is hydrolyzed into its 2 constituent monosaccharides, glucose and galactose, by β-galactosidase on the apical membrane of the intestinal enterocytes [2]. Galactose can then be absorbed and transported via the portal vein to the liver, where it is further metabolized [3] or excreted from the body. Although galactose has an identical chemical composition as glucose (both $C_6H_{12}O_6$), its structure and oxidation rate to obtain cellular energy (ATP) differ

Abbreviations: Aldob, aldolase B fructose-bisphosphate; *B2m*, beta-2 microglobulin; *Canx*, calnexin; CD163, CD163 antigen; CS, citrate synthase; En%, energy percentage; *Fbp1*, fructose bisphosphatase 1; GAL, galactose diet (16en% galactose + 16en% glucose on normal background); GLU, glucose diet (32en% glucose on normal background); GO, gene ontology; GSEA, gene set enrichment analysis; *Khk*, ketohexokinase; OXPHOS, oxidative phosphorylation; *P*.adj, adjusted *P* value; PN, postnatal day; SAA3, serum amyloid A3; TCA, tricarboxylic acid; TG, triglyceride.

* Corresponding author. *E-mail address:* evert.vanschothorst@wur.nl (E.M. van Schothorst).

https://doi.org/10.1016/j.tjnut.2023.10.011
Received 25 September 2023; Accepted 16 October 2023; Available online 18 October 2023

considerably. In order to be fully metabolized, galactose needs to be converted via several metabolic steps into glucose 6-phosphate, a glycolytic intermediate. This conversion, the Leloir pathway, occurs much slower than the phosphorylation of glucose to glucose 6-phosphate. This causes a difference in glycolytic flux and forces the cells to fully use mitochondrial oxidative phosphorylation (OXPHOS) to obtain enough energy per unit time [4]. Moreover, galactose may play a structural role, for example, during the development of the central nervous system [5].

Prolonged lactation has been associated with various health benefits [6–9], and we previously explored the hypothesis that galactose underlies these health benefits [10–12]. Galactose epimerization and further oxidation occur primarily in the liver [13]. Given the important role of the liver in galactose metabolism, we then studied the effects of this monosaccharide on hepatic metabolism and health. Using a preclinical mouse model, a postweaning diet containing glucose was compared with a diet in which part of the glucose was replaced by galactose. The postweaning galactose showed both direct and long-term health benefits. Also, mice that received galactose during the postweaning period showed lower hepatic triglyceride (TG) accumulation and inflammation [11]. Additionally, after a 9-wk high-fat diet challenge, mice that received galactose during the postweaning time presented lower total body weight, primarily because of lower adipose tissue mass and improved insulin sensitivity [10].

Although the liver is thought to be primarily responsible for galactose metabolism, the small intestine may also play a role. Recently, the intestine was shown to metabolize and clear monosaccharides, such as fructose, limiting the amount of lipogenic fructose that reaches the liver [14]. Thus, intestinal metabolism has been linked to improved liver health. The role of the intestine in galactose metabolism has not yet been investigated. Therefore, we aimed to clarify the metabolic molecular effects of galactose consumption in the small intestine. We examined the murine proximal small intestinal (jejunal) mucosa of mice exposed to a low-fat diet containing starch and monosaccharides during the immediate postweaning period. Forty-two-day-old mice fed a postweaning diet containing primarily glucose (GLU) in the monosaccharide fraction were compared with mice fed a diet in which half of the glucose was replaced by galactose (GAL). To obtain insight into the effects in the small intestine, RNA sequencing and subsequent transcriptome analysis were performed. The findings were confirmed using alternative methods (RT-qPCR) and correlated with hepatic metabolic parameters.

Methods

Animal study, diets, and tissue acquisition

The animal study and the diets used were previously described in detail [11]. Briefly, from standardized nests, on postnatal day (PN) 21, offspring C57BL/6JRccHsd mice were stratified by body weight and received 1 of 2 diets for 3 wk while in individual housing (n = 12 per diet group and sex). The diets contained 16energy percentage (en%) fat, 20en% protein, and 64en% carbohydrate, including 29en% starch and 35en% monosaccharides, of which 3en% was fructose and the remainder were either glucose (GLU; 32en% glucose) or glucose and galactose (GAL; 16en% galactose and 16en% glucose) (Figure 1, Supplemental Table 1). The GAL diet thus mimics lactose; however, the constituent components were provided separately to prevent potential lactose-induced diarrhea after weaning. Here, we studied female mice because the long-term beneficial effects were observed in this sex [10]. On day 42, mice were starved for 2–5 h and killed by decapitation. The intestine was taken and carefully rinsed in cold (4°C) phosphate-buffered saline to remove any potential contaminants. The first proximal 3 cm was excised and discarded. The remaining small intestine was then divided into 2 equal-length segments and scraped. The scrapings were immediately snap-frozen in liquid nitrogen and stored at −80°C until further analysis. The proximal part, corresponding with the first half of the jejunum, was used for all the analyses.

RNA isolation and RNA sequencing

Total RNA was isolated from the scrapings using the RNeasy mini kit (Qiagen). The integrity of RNA was checked using an Agilent 2200 Tape Station system (Agilent Technologies). All but one sample passed the A230/260, A260/280, and integrity quality controls. Strand-specific transcriptome resequencing was performed on total RNA isolated from proximal intestine scrapings. RNA preparation, library construction, and sequencing using DNBSEQ technology were performed at the Beijing Genomics Institute. Clean and filtered reads were obtained in the FASTQ format, and a quality check was performed using FASTQC [15]. The reads were aligned to the mouse genome (GRCm39.104) using STAR [16], and counts were performed using HTSeq [17]. The average sequencing depth was 17.3 M paired-end reads, of which $\geq$83.5% were uniquely mapped.

Transcriptome analysis

Data and statistical analyses were performed using the statistical software R version 4.1.0. DESeq2 [18] was used to identify differentially expressed genes between the mice fed GAL (n = 12) and GLU (n = 11). An extra filtering step with the removal of genes with <10 reads per row was applied. Benjamini–Hochberg multiple-testing correction was used to obtain adjusted P values (P.adj) at a false discovery rate of 10%. Volcano plots were constructed using rlog-transformed data with library size correction. All data were deposited in the Gene Expression Omnibus dataset GSE183792.

Gene Ontology enrichment analyses

Gene Ontology (GO) enrichment analysis (enrichGO) for biological processes was performed in R using ClusterProfiler [19]. Only significant transcripts were used for the analysis with a P.adj of < 0.1. Additionally, we used the mouse MitoCarta database [20] as a reference inventory for mitochondrial transcripts. Gene set enrichment analysis (GSEA) was performed to investigate cellular components, and the resulting components were semantically clustered in a tree plot.

Quantitative RT-PCR

Transcript expression validation of the RNAseq was measured using iQ SYBR Green Supermix (Bio-Rad) on a CFX96 Touch Real-Time PCR Detection System (Bio-Rad), with 3 min at 95°C, 40 cycles of 15 s at 95°C, and 45 s at the annealing and elongation temperatures, followed by melt-curve analysis. Primers were designed using NCBI Primer-Blast (NCBI website); an overview of primer sequences and annealing temperatures is

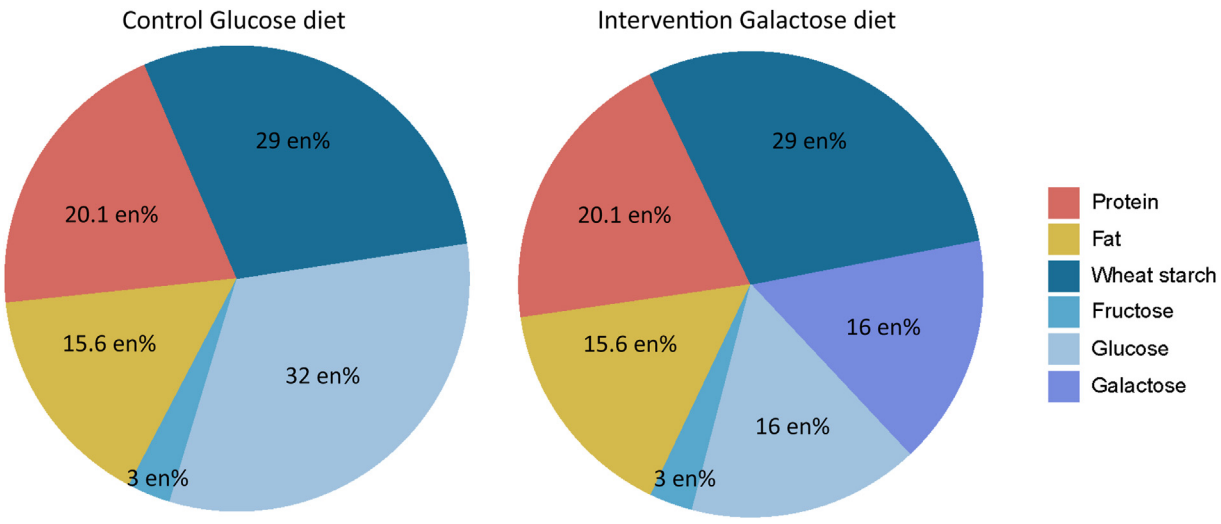

FIGURE 1. Diet composition overview. Both control-GLU (left) and intervention-GAL (right) diets had an overall composition of 64en% carbohydrates, 15.6en% fat, and 20.1en% protein. For the carbohydrate fraction, fructose accounted for only 3en% and wheat starch 29en% in both diets; the remaining 32en% came from glucose in the GLU diet and 16en% glucose + 16en% galactose in the GAL diet. En%, energy percentage; GAL, galactose diet; GLU, glucose diet.

given in Supplemental Table 2. cDNA from all samples was pooled, and serial dilutions were used for standard curves; for each transcript, 2 negative controls were also included (water and a sample without reverse transcriptase). Samples were measured in a 100-fold dilution; samples and standards were measured in duplicate. Stable gene expression levels were determined using Bio-Rad CFX Maestro software (version 4.1; Bio-Rad), and data were normalized against stable reference genes, namely Calnexin (*Canx*) and β-2 microglobulin (*B2m*).

Citrate synthase assay

Mitochondrial citrate synthase (CS) activity level as a proxy for mitochondrial mass was determined using the CS assay kit (Sigma-Aldrich) according to the manufacturer's instructions. Values were calculated with an extinction coefficient of 13.6 / (mM × cm) and normalized to the protein content, which was measured using the DC protein assay kit (Bio-Rad Laboratories), according to the manufacturer's instructions.

Liver TG measurements and serum SAA3 measurement

Previously, liver TG concentrations in the right lobe were determined using the Liquicolor TG kit (Human) [11]. Likewise, circulating serum amyloid A3 (SAA3) concentrations were measured using the mouse SAA3 ELISA kit (Merck chemicals B.V.) according to the manufacturer's instructions [11]. Here, we used these molecular data to analyze the correlations between intestinal transcript levels and these hepatic parameters per mouse.

Histologic analysis

The liver fixed in 4% paraformaldehyde for 24 h at 4°C was embedded in paraffin blocks and cut into 5-μm-thick sections. Sections were dewaxed in xylene and rehydrated for staining. An epitope-specific antibody was used for the detection and quantification of CD163 (1:200; 182422 Abcam). After rehydration, sections were washed with tris-buffered saline and the antigen was retrieved using 10mM sodium citrate, pH 6.0 for 10 min at sub-boiling temperatures in the microwave. Sections were left to cool for 30 min at room temperature and washed 5 times for 5 min each with tris-buffered saline. Tissue sections were blocked with 5% goat serum (S-1000, Vector Laboratories) for 30 min at room temperature. The sections were then incubated with the primary antibody overnight at 4°C. Before incubation with the secondary antibody, the sections were treated with 1% Sudan black (199664; Sigma-Aldrich) diluted in 70% ethanol for 10 min and then washed under a demi-water tap for 5 s per slide. The sections were incubated with the diluted secondary antibody Alexa 488 goat anti-rabbit (1:200; A11008; Invitrogen) for 1 h at room temperature. The nuclei were stained with 4′,6-diamidino-2-phenylindole (DAPI; 1:10,000; D9564; Sigma-Aldrich) for 5 min at room temperature; secondary controls and IgG (Vector Laboratories) controls at the same concentration as the primary antibody were used to correct for nonspecific binding. Sections were then mounted with Fluoromount-G (0100-01; Southern Biotech) and dried in the dark at 4°C overnight.

Image acquisition processing and quantification

The images were taken with a Leica DM6b microscope (Leica Micro Systems Inc.). To get a full representation of the section, the tile-scan mode was used; with this function, 350–600 consecutive pictures were taken and then stitched together.

The number of CD163-positive cells ($CD163^+$) per tissue was obtained using the ImageJ software version 1.52i. To correct for individual pixels that were fluorescent due to artifacts and based on the observed size of clearly positive cells, the size of the $CD163^+$ cells was estimated to be between 20 and 200 μm^2. Based on this quantification, the final data are given as the number of $CD163^+$ cells per 10,000 μm^2.

Statistical analysis

Differentially expressed gene (DEG) and pathway analyses were performed using R version 4.1.0. Analyses of transcript levels are described above. Pearson correlation analysis was performed using

GraphPad Prism version 9.31 (GraphPad Software). *P* values and *R* coefficients are indicated in each figure panel.

Results

Postweaning galactose consumption affects mitochondrial metabolism in the proximal small intestinal mucosa

In a previous study, we demonstrated the positive metabolic effects of postweaning galactose consumption in mice, including lower hepatic TG concentrations, despite having significantly higher cumulative food intake in the GAL group, with similar body weight, lean mass, and fat mass [11]. In line with the reduced lipid accumulation, galactose consumption reduced hepatic inflammation and liver-secreted concentrations of the circulatory inflammatory marker SAA3 [11]. Immunohistochemistry of the liver sections showed a significant decrease in $CD163^+$ cells, identifiable as Kupffer cells in the mice fed GAL (Figure 2A–D). The number of $CD163^+$ cells was positively correlated with the hepatic transcript levels of *Saa3* (Figure 2E). Building on these findings, we hypothesized that the positive effects of galactose consumption seen in the liver might be due to primary alterations in the small intestine and the effects seen in the liver could be secondary. To investigate this hypothesis, RNA sequencing was performed using intestinal mucosal scrapings from these mice. Of >20,000 transcripts, 301 ($P.adj < 0.1$) were significantly affected by dietary galactose. Pathway analysis using GO enrichment showed that the 10 most upregulated pathways were all related to cellular energy production and metabolism, with a clear predominance of mitochondrial metabolic pathways (Figure 3A). Subsequent GSEA for cellular components confirmed the predominant role of the intervention on genes involved in mitochondrial metabolism (Figure 3B). Focusing specifically on mitochondrial transcripts, ~26% of the differentially regulated transcripts were mitochondrially allocated, and >90% of them were upregulated by galactose consumption (Figure 3C, Supplemental Tables 3, 4).

Postweaning galactose consumption increases OXPHOS expression

Given that mitochondrial transcripts were prominently upregulated and mitochondrial metabolic processes appeared as some of the top-regulated processes, mitochondrial pathways were further investigated to gain a better understanding of their specific contributions. This revealed that the main upregulated process in the mitochondria was ATP production, with this increase almost exclusively attributable to OXPHOS metabolism (Figure 3A). Selecting all OXPHOS genes from the MitoCarta 3.0 gene set, which represents all verified mitochondrial genes, we observed that these transcripts were exclusively and consistently upregulated, regardless of significance (Supplemental Figure 1). Additionally, when focusing on the specific genes, all 5 complexes of the OXPHOS system showed significant upregulation of several subunits, whereas none were downregulated (Figure 4, Supplemental Table 5). Notably, CS is considered a marker of

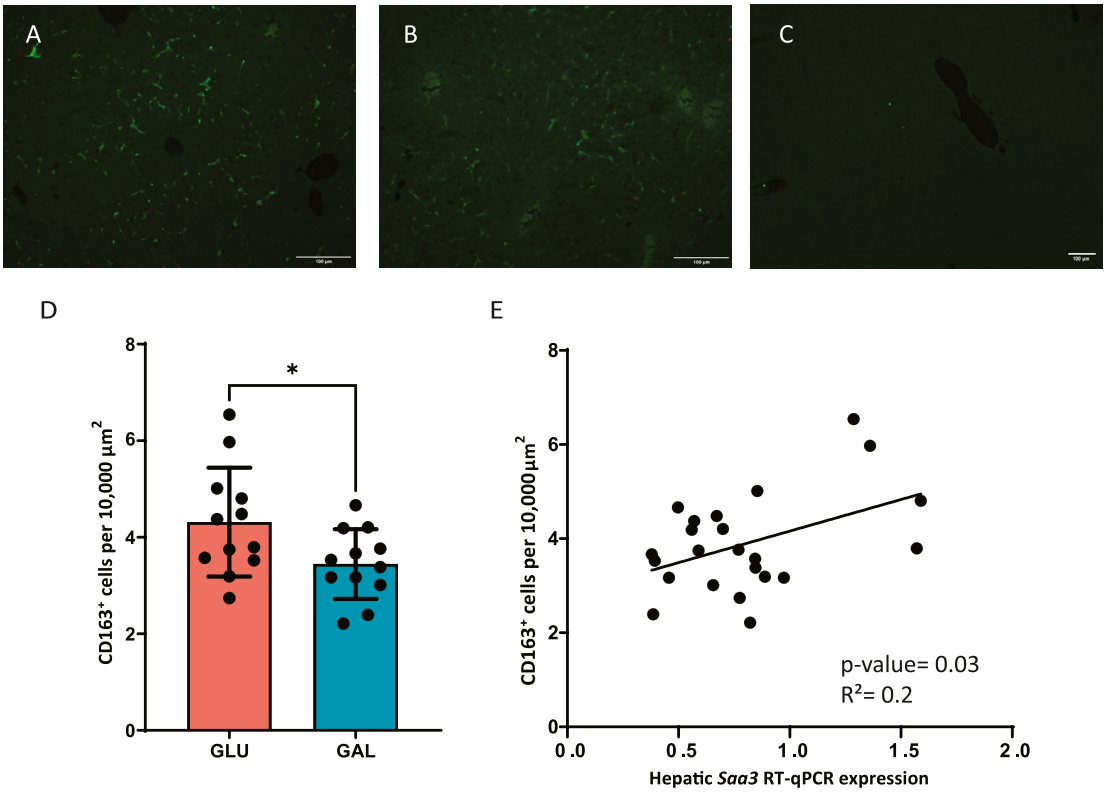

FIGURE 2. Immunofluorescent staining of hepatic sections against CD163. (A, B) A randomly picked section at 200x magnification of a control-GLU and an intervention-GAL-fed mouse. (C) The negative control using rabbit immunoglobulin at 100× magnification. Sections were scanned completely and the number of $CD163^+$ cells over the entire surface of the section was obtained and divided per 10,000 μm^2. (D) A significant reduction in the number of $CD163^+$ cells was observed in the GAL group. Additionally, the number of $CD163^+$ cells was positively correlated with the hepatic expression of *Saa3*. Scale bars represent 100 µm. CD163, CD163 antigen; GAL, galactose diet; GLU, glucose diet; SAA3, serum amyloid A3.

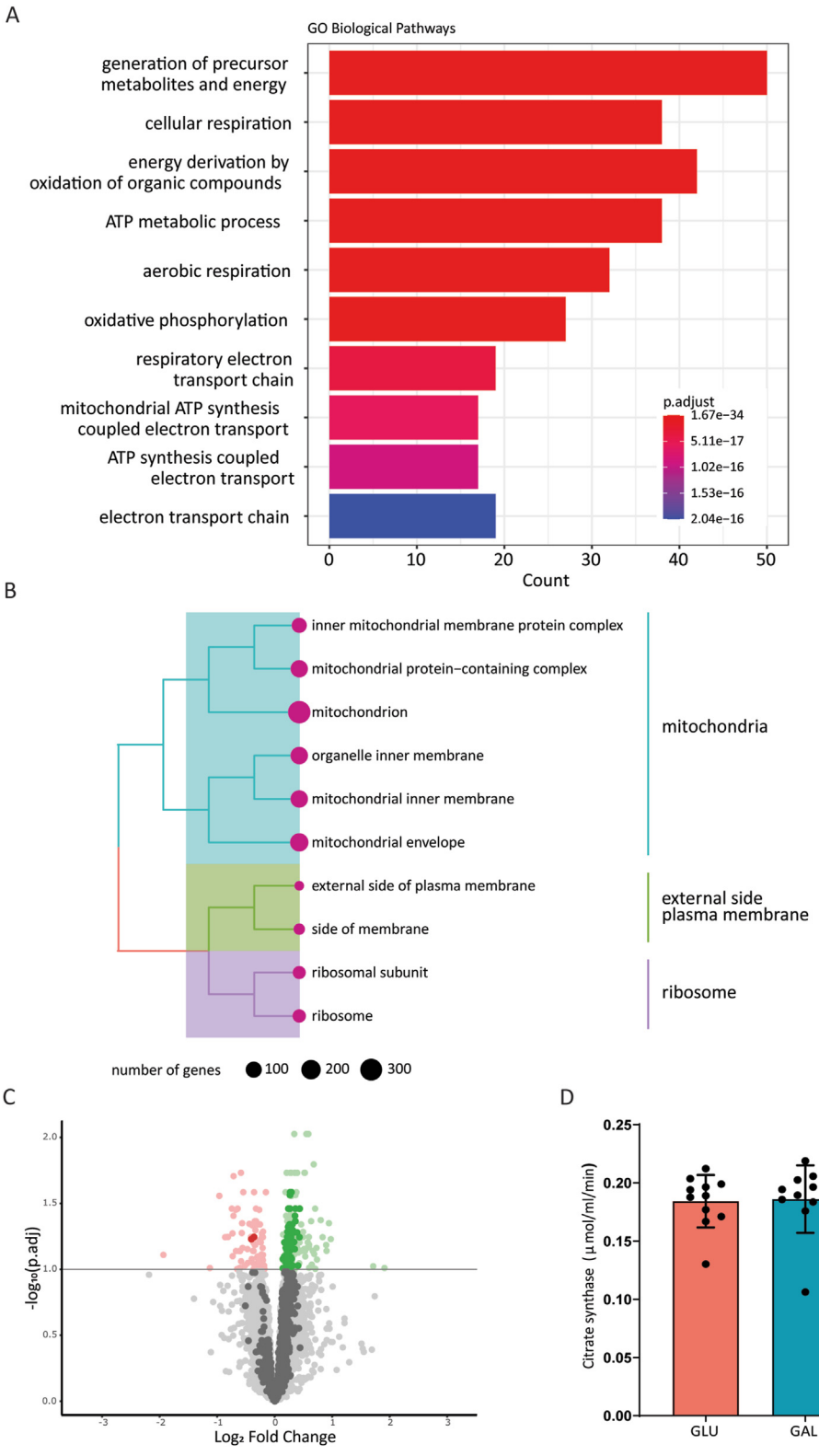

(caption on next page)

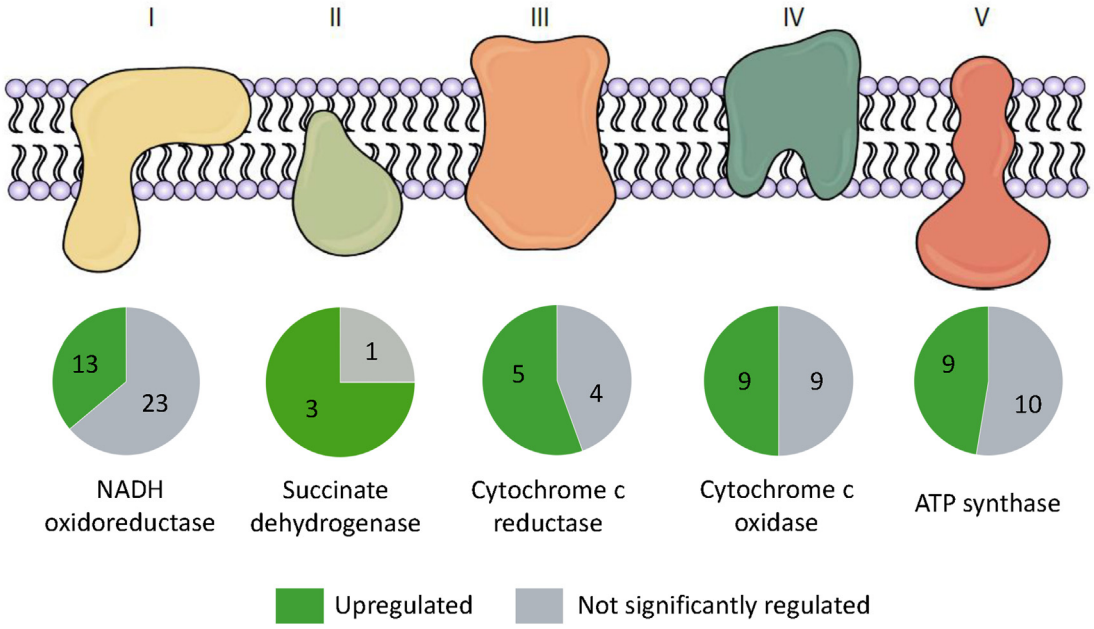

FIGURE 4. Diagram of OXPHOS complexes with a representation of transcript regulation. All individual complexes of OXPHOS (1–5) had a high percentage of significantly regulated genes, all of them being upregulated and none downregulated, independent of significance. OXPHOS, oxidative phosphorylation.

mitochondrial mass; yet, both gene expression and protein concentrations of CS remained unaffected (Figure 2D), suggesting that the increase in OXPHOS is not due to an increase in the mitochondrial mass. In contrast, several transcripts encoding mitochondrial ribosomal proteins, which are nuclear-encoded, were significantly upregulated (data not shown), indicating increased mitochondrial protein synthesis without changes in mass. Moreover, no significant effects were found in other mitochondrial pathways, such as the tricarboxylic acid (TCA) cycle or fatty acid β-oxidation.

Postweaning galactose consumption increases glycolysis and fructolysis without upregulating the TCA cycle

Besides mitochondrial energy metabolism, pathway analysis also revealed that monosaccharide metabolism was significantly upregulated, which was expected based on the monosaccharide nutritional intervention. However, most transcripts involved in glucose metabolism were significantly upregulated by the presence of galactose; thus, when less glucose was present in the diet (Figure 5A). The expression of a selection of these transcripts was validated using RT-qPCR; all the transcripts showed a significant correlation of the normalized RT-qPCR expression with the RNAseq normalized counts (Supplemental Figure 2). Intestinal galactose catabolism-specific transcripts, reflecting the metabolism of galactose to the glycolysis intermediate glucose 6-P, appeared nonsignificantly regulated (Figure 5A). Thus, the increase in OXPHOS expression coincides with an upregulation of glycolysis-encoded transcripts. Moreover, despite an identical amount of fructose being present in the control and intervention diets, and fructose only representing ~3% of the total dietary energy, the presence of dietary galactose caused a consistent significant upregulation of the main fructolytic enzymes (Figure 5A). Fructose has been considered a hepatic lipogenic factor, and it was already reported that the galactose intervention could reduce the content of hepatic TG ($P = 0.03$), with a 30% difference in the hepatic TG content between the 2 groups [11]. Importantly, the intestinal transcripts involved in fructose metabolism (*KhK, Aldob,* and *Fbp1*) and downstream glycolysis (*Gapdh*) were all negatively correlated with the TG content in the liver (Figure 5B, Supplemental Figure 3). Furthermore, the expression of all differentially expressed cytoplasmic monosaccharide metabolism transcripts in the small intestinal mucosa was negatively correlated with circulating levels of the liver-secreted inflammatory marker SAA3 (Figure 5C, Supplemental Figure 4), which were decreased ($P = 0.03$) by 21% in the galactose-fed animals, as reported previously [11]. Here, we enforce this by showing a decrease in $CD163^{+}$ cells. The strong negative correlation between intestinal fructose-metabolism genes and hepatic lipid concentrations suggests a strong connection between intestinal substrate utilization and hepatic physiology.

FIGURE 3. Overview of the mitochondrial effects of dietary intervention in the intestinal mucosa. (A) Top 10 most (up)regulated pathways using GO enrichment analysis of small intestinal mucosal differentially expressed transcripts (*P*.adj < 0.1) comparing galactose and control glucose. (B) GSEA for the cellular component. The diagram depicts the 10 most frequent cellular components associated with the DEG. Clustering was performed based on semantic overlap. (C) Volcano plot of the ratio of GAL/GLU vs. *P*.adj value displaying all genes in light (grey) color and genes encoding mitochondrial proteins on top in dark (grey). Red indicates downregulation in the galactose group, whereas light/dark green indicates upregulation. The horizontal line indicates the threshold for significance (*P*.adj < 0.1). (D) Mitochondrial mass as measured by CS assay of the control glucose group (GLU, $n = 11$) and galactose group (GAL, $n = 11$). Values are expressed as mean ± SD. CS, citrate synthase; DEG, differentially expressed gene; GAL, galactose diet; GLU, glucose diet; GO, gene ontology; GSEA, gene set enrichment analysis; *P*.adj, adjusted *P* value.

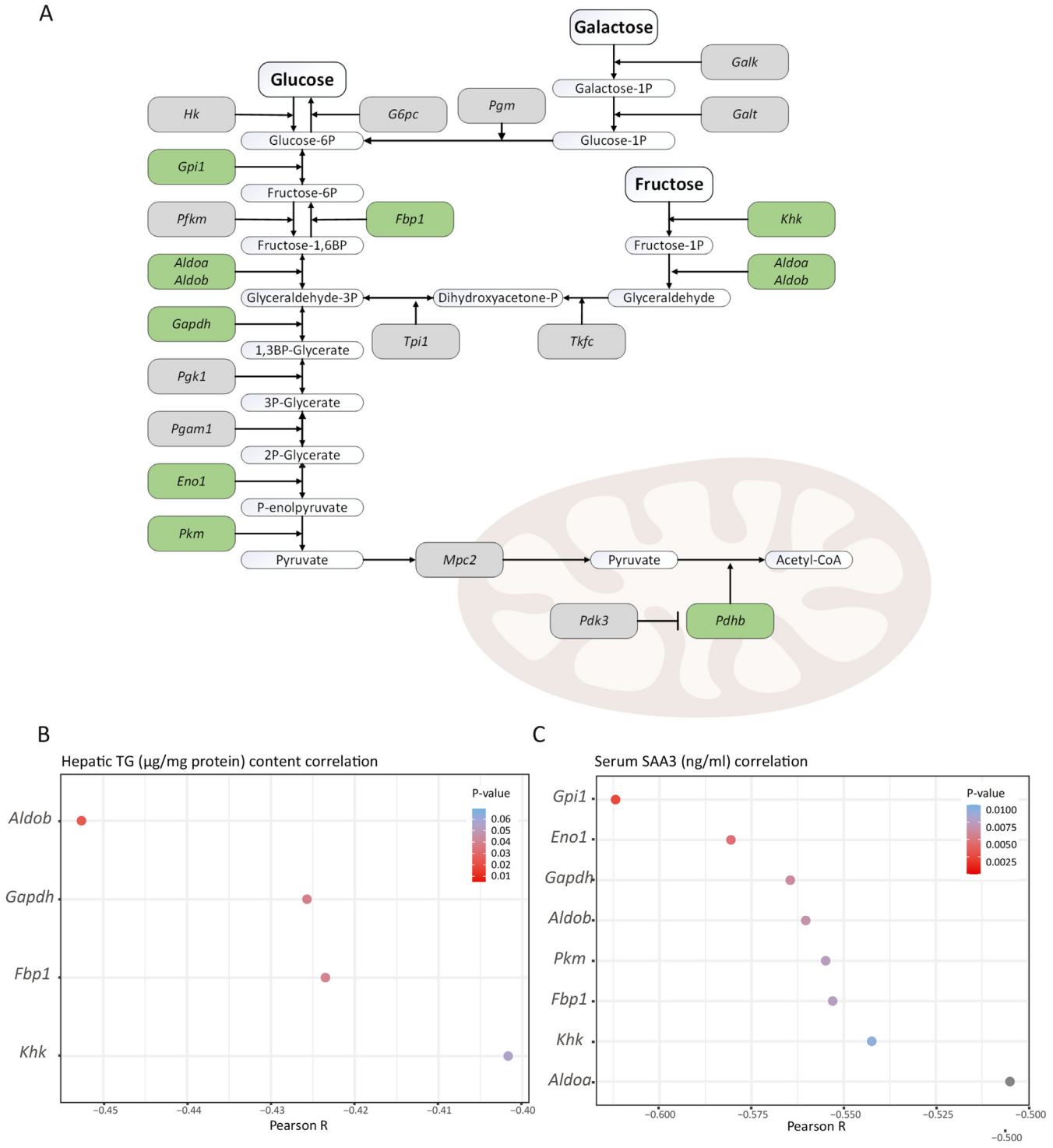

FIGURE 5. Glucose and fructose-metabolism pathways and their correlation with circulating SAA3 and hepatic TG content. (A) Cellular glucose, galactose, and fructose-metabolism pathways in cytoplasm and mitochondria. Color coding of transcripts indicates upregulation (significant in green, nonsignificant in grey). (B) Pearson R correlation coefficients and associated *P* value of selected significantly regulated transcripts against hepatic TG concentrations expressed as μg TG/mg protein and (C) serum SAA3 concentrations expressed as ng SAA3/mL serum. Selected significant transcripts shown in green in panel 4A were used for correlation analysis. SAA3, serum amyloid A3; TG, triglyceride.

Discussion

The effects of partially replacing postweaning dietary glucose with galactose were investigated for its effects on intestinal tissue and the underlying mechanism. OXPHOS appeared as the top-upregulated process, along with cytoplasmic carbohydrate metabolism. Moreover, the expression of key metabolic transcripts in the small intestinal mucosa was negatively correlated

with hepatic metabolic markers, such as hepatic TGs, Kupffer cells, and circulating concentrations of SAA3. Our study, by feeding the weaned mice galactose and glucose in an equimolar ratio, aimed to mimic from a carbohydrate point of view, a situation of prolonged breastfeeding or milk intake, which has been repeatedly reported to be beneficial by the WHO and numerous studies [6–9]. Our data suggest that intestinal carbohydrate metabolism may contribute to this, at least impacting liver health.

After feeding GAL, energy metabolism was the most regulated process in the small intestinal mucosa (Figure 3A). This effect was further confirmed using GSEA for cellular components (Figure 3B). Additionally, further analysis of the mitochondrial transcripts showed that the vast majority of them were upregulated regardless of their significance (Figure 3C, Supplemental Table 2). Other key mitochondrial metabolic processes, such as the TCA cycle and fatty acid β-oxidation, were not regulated, and neither was the mitochondrial mass (Figure 3D), cumulatively indicating that OXPHOS was specifically upregulated by galactose in the diet. This in vivo observation confirms in vitro findings in intestinal, muscle, and liver cell cultures, which turn on their OXPHOS machinery upon replacement of glucose with galactose in the culture media [21–23]. This may be due to the lower glycolytic flux of galactose to pyruvate compared with the conversion of glucose to pyruvate, reversing the glycolytic phenotype of the in vitro cultured cell lines toward a more OXPHOS-relying state to fulfill their energy needs [4]. The upregulated OXPHOS genes corresponded to all 5 complexes (Figure 4). Notably, although the nuclear-encoded mitochondrial OXPHOS transcripts were greatly affected, none of the 13 mitochondrial-encoded transcripts showed any significant differential expression. Besides the OXPHOS-encoding genes, transcripts encoding several mitochondrial ribosomal proteins were upregulated, indicating an increase in mitochondrial protein synthesis, which has previously been positively associated with OXPHOS function [24,25].

The decreased glycolytic flux induced by dietary galactose resembles a state of energy deprivation. To see whether this would be similar to caloric restriction, we further compared our galactose-induced transcript effects to those seen by caloric restriction in murine intestines [26; ArrayExpress dataset E-MTAB-6248] but observed no overt overlap, with only a few overlapping differentially expressed transcripts and no overlap at the pathway level. This at least suggests that galactose-induced effects are different from calorie restriction-induced effects. This could be partially attributable to the metabolic state of the tissues, which were collected from the mice 5 h after food deprivation; thus, at the end of the postprandial phase or start of the postabsorptive phase, which might be different from caloric-restricted mice that were usually in the fully fasted state when sampled.

Although mitochondrial OXPHOS was the most affected process, cytoplasmic carbohydrate metabolism was also substantially affected. All transcripts for glycolysis and fructose to glucose conversion were upregulated, most of them significantly so, cumulatively indicating enhancement of the entire pathway (Figure 5A). Furthermore, the main fructolytic enzymes and regulators of fructose metabolism were upregulated in the GAL group, although the amount of fructose in the GAL diet was not different from that in the GLU diet and there were no differences in the food intake [11]. This suggests an increased fructose catabolism in enterocytes. This may be attributed to fructose being a faster metabolic substrate than galactose [27].

Fructose is a topic of interest because many studies have linked excessive fructose intake to liver steatosis and inflammation in mice [28–30] and humans [31]. Fructose can already have detrimental effects in moderate doses ranging from 1 to 4 g of fructose/kg body weight [32,33]. Previous work by Jang et al. [14] showed that a single gavage of fructose at a dose of 1 g /kg body weight was sufficient to induce hepatic lipogenic effects. In our intervention, the dietary fructose fraction represented only 3% of the total caloric intake, which cannot be considered a high-fructose diet. Nevertheless, this may impact the liver, as the daily intake of fructose was around 4.6 g of fructose/kg body weight, and the cumulative effect over 3 wk, despite not being pathologic, would be sufficient to trigger the observed hepatic effects, even more so in the context of a relatively high monosaccharide background (35% of the total caloric intake was monosaccharides). It is important to emphasize that our control mice represent a healthy status, and we hypothesized that the galactose intervention had a further health-promoting effect. Therefore, we did not expect liver pathology or injury. This is further confirmed by the absence of differences in the serum concentrations of alanine transaminase [11], a classic hepatic damage marker [34].

Although the mice were not diseased, we previously observed a notable decrease in the expression of immune-related genes after the 3-wk GAL intervention [11]. Interestingly, a majority of the top downregulated pathways in the liver were associated with inflammatory processes. One gene that particularly stood out as significantly downregulated was *Saa3*, a well-established marker of hepatic inflammation. This downregulation was evident at both the transcript level in the liver and the protein level in circulation. SAA3 is primarily secreted by macrophages, with Kupffer cells being the predominant hepatic macrophages in nondisease conditions [35,36]. We also observed a significant decrease in the number of $CD163^{+}$ cells, possibly Kupffer cells [35], in the GAL group (Figure 2A–D), which was positively correlated with the hepatic transcript expression of *Saa3* (Figure 2E).

In the small intestinal mucosa, we showed that galactose-induced upregulation of the expression of all significant cytoplasmatic transcripts involved in glucose and fructose metabolism was negatively correlated with circulating SAA3. Moreover, the increased expression of several intestinal fructolytic enzymes in GAL mice was negatively correlated with hepatic TG content. These results are fully aligned with a recent study that revealed that functional intestinal fructose catabolism shields the liver from fructose-induced damage by decreasing the amount of fructose that eventually reaches the liver [14]. Additionally, tissue-specific knockout of intestinal fructolytic enzymes led to increased hepatic steatosis, whereas the overexpression had a fructose-clearance effect in the small intestine, resulting in decreased hepatic fructose-induced lipogenesis [14]. It is tempting to speculate that galactose intake might contribute to shielding the liver from fructose-induced damage. It needs to be confirmed whether this potential galactose-induced fructose shielding also occurs when the galactose-containing disaccharide lactose is consumed. If so, fructose shielding by galactose may explain part of the health benefits of extended breastfeeding, besides other key milk

components, such as milk oligosaccharides and immune factors present in breast milk, which have been endowed with health benefits [37,38].

This study focused on female mice, because, contrary to male mice, beneficial programing effects were seen in this sex. With an increasing number of studies analyzing both sexes, sexual dimorphic metabolic responses are frequently observed [39,40]. The causes underlying these sex differences are less clear and may be due to differences in body composition, blood circulation, or other developmental differences, or may be a direct consequence of sex-related differences in steroid hormones.

Overall, our findings suggest that changes in energy metabolism in the small intestinal mucosa might be linked to liver health. Several studies have shown how changes in the intestinal barrier, inflammation, or even the microbiota in the small intestine are directly linked to liver health [41,42]. Here, we show that the metabolic pathways and substrate utilization in the small intestinal mucosa can also be correlated to hepatic function and physiology. Thus, modulating the small intestine energy metabolism pathways with dietary interventions, as we have shown now for galactose, can result in improved metabolic status beyond intestinal health.

Acknowledgments

We thank the staff of the CARUS facility for their assistance in the execution of the animal experiments, and Mette Ekkel for her contribution to the experiments.

Author contributions

The authors' responsibilities were as follows – FSFC, LMSB, JK, EMvS: designed the research; FSFC: performed the experiments; FSFC, EMvS: analyzed the data; FSFC, LMSB, EMvS, JK: wrote the draft and the final manuscript; FSFC: took primary responsibility for the final content; and all authors: read and approved the final manuscript.

Conflicts of Interest

The authors declare no conflicts of interest.

Funding

This project was partly funded by TKI – TopSector Agri & Food, project number LWV20.387.

Data availability

Data described in the manuscript, code book, and analytic code will be made available upon reasonable request.

Appendix A. Supplementary data

Supplementary data to this article can be found online at https://doi.org/10.1016/j.tjnut.2023.10.011.

References

[1] A. Stephen, M. Alles, C. de Graaf, M. Fleith, E. Hadjilucas, E. Isaacs, et al., The role and requirements of digestible dietary carbohydrates in infants and toddlers, Eur. J. Clin. Nutr. 66 (2012) 765–779, https://doi.org/10.1038/ejcn.2012.27.

[2] K. Takata, Glucose transporters in the transepithelial transport of glucose, J. Electron Microsc. (Tokyo) 45 (4) (1996) 275–284, https://doi.org/10.1093/oxfordjournals.jmicro.a023443.

[3] E.M. Wright, Glucose transport families SLC5 and SLC50, Mol. Aspects Med 34 (2–3) (2013) 183–196, https://doi.org/10.1016/j.mam.2012.11.002.

[4] R. Rossignol, R. Gilkerson, R. Aggeler, K. Yamagata, S.J. Remington, R.A. Capaldi, Energy substrate modulates mitochondrial structure and oxidative capacity in cancer cells, Cancer Res 64 (3) (2004) 985–993, https://doi.org/10.1158/0008-5472.CAN-03-1101.

[5] K.G. Petry, J.K.V. Reichardt, The fundamental importance of human galactose metabolism: lessons from genetics and biochemistry, Trends Genet 14 (3) (1998) 98–102, https://doi.org/10.1016/S0168-9525(97)01379-6.

[6] C.J. Stewart, N.J. Ajami, J.L. O'Brien, D.S. Hutchinson, D.P. Smith, M.C. Wong, et al., Temporal development of the gut microbiome in early childhood from the TEDDY study, Nature 562 (2018) 583–588, https://doi.org/10.1038/s41586-018-0617-x.

[7] A. Pietrobelli, M. Agosti, Nutrition in the first 1000 days: ten practices to minimize obesity emerging from published science, Int. J. Environ. Res. Public Health. 14 (12) (2017) 1491, https://doi.org/10.3390/ijerph14121491.

[8] World Health Organization, Complementary feeding: report of the global consultation, and summary of guiding principles for complementary feeding of the breastfed child [Internet], 2002 [accessed 28 February 2023]. Available from: https://www.who.int/publications/i/item/924154614X.

[9] V. Pena-Leon, C. Folgueira, S. Barja-Fernández, R. Pérez-Lois, N. Da Silva Lima, M. Martin, et al., Prolonged breastfeeding protects from obesity by hypothalamic action of hepatic FGF21, Nat. Metab. 4 (2022) 901–917, https://doi.org/10.1038/s42255-022-00602-z.

[10] L.M.S. Bouwman, J.M.S. Fernández-Calleja, I. van der Stelt, A. Oosting, J. Keijer, E.M. van Schothorst, Replacing part of glucose with galactose in the postweaning diet protects female but not male mice from high-fat diet–induced adiposity in later life, J. Nutr. 149 (7) (2019) 1140–1148, https://doi.org/10.1016/j.jnutbio.2019.108223.

[11] L.M.S. Bouwman, H.J.M. Swarts, J.M.S. Fernández-Calleja, I. van der Stelt, H. Schols, A. Oosting, et al., Partial replacement of glucose by galactose in the post-weaning diet improves parameters of hepatic health, J. Nutr. Biochem. 73 (2019) 108223, https://doi.org/10.1016/j.jnutbio.2019.108223.

[12] P. Sun, L.M.S. Bouwman, J.L. de Deugd, I. van der Stelt, A. Oosting, J. Keijer, et al., Galactose in the post-weaning diet programs improved circulating adiponectin concentrations and skeletal muscle insulin signaling, Int. J. Mol. Sci. 23 (18) (2022) 10207, https://doi.org/10.3390/ijms231810207.

[13] H.M. Holden, I. Rayment, J.B. Thoden, Structure and function of enzymes of the leloir pathway for galactose metabolism, J. Biol. Chem. 278 (45) (2003) 43885–43888, https://doi.org/10.1074/jbc.R300025200.

[14] C. Jang, S. Wada, S. Yang, B. Gosis, X. Zeng, Z. Zhang, et al., The small intestine shields the liver from fructose-induced steatosis, Nat. Metab. 2 (2020) 586–593, https://doi.org/10.1038/s42255-020-0222-9.

[15] S. Andrews, FastQC: quality control tool for high throughput sequence data [Internet], 2010 [accessed 3 February 2023]. Available from: http://www.bioinformatics.babraham.ac.uk/projects/fastqc/.

[16] A. Dobin, C.A. Davis, F. Schlesinger, J. Drenkow, C. Zaleski, S. Jha, et al., STAR: ultrafast universal RNA-seq aligner, Bioinformatics 29 (1) (2013) 15–21, https://doi.org/10.1093/bioinformatics/bts635.

[17] S. Anders, P.T. Pyl, W. Huber, HTSeq—a Python framework to work with high-throughput sequencing data, Bioinformatics 31 (2) (2015) 166–169, https://doi.org/10.1093/bioinformatics/btu638.

[18] M.I. Love, W. Huber, S. Anders, Moderated estimation of fold change and dispersion for RNA-seq data with DESeq2, Genome Biol 15 (2014) 550, https://doi.org/10.1186/s13059-014-0550-8.

[19] G. Yu, L.G. Wang, Y. Han, Q.Y. He, ClusterProfiler: an R package for comparing biological themes among gene clusters, Omics. J. Integr.. Biol. 16 (5) (2012) 284–287, https://doi.org/10.1089/omi.2011.0118.
[20] S. Rath, R. Sharma, R. Gupta, T. Ast, C. Chan, T.J. Durham, et al., MitoCarta3.0: an updated mitochondrial proteome now with sub-organelle localization and pathway annotations, Nucleic Acids Res 49 (D1) (2021) D1541–D1547, https://doi.org/10.1093/nar/gkaa1011.
[21] L.M. JanssenDuijghuijsen, S. Grefte, V.C.J. de Boer, L. Zeper, D.A.M. van Dartel, I. van der Stelt, et al., Mitochondrial ATP depletion disrupts Caco-2 monolayer integrity and internalizes claudin 7, Front. Physiol. 8 (2017) 794, https://doi.org/10.3389/fphys.2017.00794.
[22] C. Aguer, D. Gambarotta, R.J. Mailloux, C. Moffat, R. Dent, R. McPherson, et al., Galactose enhances oxidative metabolism and reveals mitochondrial dysfunction in human primary muscle cells, PLoS. One. 6 (12) (2011) e28536, https://doi.org/10.1371/journal.pone.0028536.
[23] R.A. Skolik, J. Solocinski, M.E. Konkle, N. Chakraborty, M.A. Menze, Global changes to HepG2 cell metabolism in response to galactose treatment, Am. J. Physiol. Cell Physiol. 320 (5) (2021) C778–C793, https://doi.org/10.1152/ajpcell.00460.2020.
[24] S. Heinonen, J. Buzkova, M. Muniandy, R. Kaksonen, M. Ollikainen, K. Ismail, et al., Impaired mitochondrial biogenesis in adipose tissue in acquired obesity, Diabetes 64 (9) (2015) 3135–3145, https://doi.org/10.2337/db14-1937.
[25] K.L. Perks, N. Ferreira, T.R. Richman, J.A. Ermer, I. Kuznetsova, A.J. Shearwood, et al., Adult-onset obesity is triggered by impaired mitochondrial gene expression, Sci. Adv. 3 (8) (2017) e1700677, https://doi.org/10.1126/sciadv.1700677.
[26] K. Duszka, S. Ellero-Simatos, G.S. Ow, M. Defernez, E. Paramalingam, A. Tett, et al., Complementary intestinal mucosa and microbiota responses to caloric restriction, Sci. Rep. 8 (2018) 11338, https://doi.org/10.1038/s41598-018-29815-7.
[27] S.Z. Sun, M.W. Empie, Fructose metabolism in humans - what isotopic tracer studies tell us, Nutr. Metab. (Lond.) 9 (2012) 89, https://doi.org/10.1186/1743-7075-9-89.
[28] T. Jensen, M.F. Abdelmalek, S. Sullivan, K.J. Nadeau, M. Green, C. Roncal, et al., Fructose and sugar: a major mediator of non-alcoholic fatty liver disease, J. Hepatol. 68 (2018) 1063–1075, https://doi.org/10.1016/j.jhep.2018.01.019.
[29] M.B. Vos, J.E. Lavine, Dietary fructose in nonalcoholic fatty liver disease, Hepatology 57 (6) (2013) 2525–2531, https://doi.org/10.1002/hep.26299.
[30] N. Mamikutty, Z.C. Thent, F. Haji Suhaimi, Fructose-drinking water induced nonalcoholic fatty liver disease and ultrastructural alteration of hepatocyte mitochondria in male Wistar rat, Biomed. Res. Int. 2015 (2015) 895961, https://doi.org/10.1155/2015/895961.
[31] J.S. Lim, M. Mietus-Snyder, A. Valente, J.M. Schwarz, R.H. Lustig, The role of fructose in the pathogenesis of NAFLD and the metabolic syndrome, Nat. Rev. Gastroenterol. Hepatol. 7 (2010) 251–264, https://doi.org/10.1038/nrgastro.2010.41.
[32] I. Aeberli, M. Hochuli, P.A. Gerber, L. Sze, S.B. Murer, L. Tappy, et al., Moderate amounts of fructose consumption impair insulin sensitivity in healthy young men: a randomized controlled trial, Diabetes Care 36 (1) (2013) 150–156, https://doi.org/10.2337/dc12-0540.
[33] V. Lecoultre, L. Egli, G. Carrel, F. Theytaz, R. Kreis, P. Schneiter, et al., Effects of fructose and glucose overfeeding on hepatic insulin sensitivity and intrahepatic lipids in healthy humans, Obesity (Silver Spring) 21 (4) (2013) 782–785, https://doi.org/10.1002/oby.20377.
[34] R.K. Schindhelm, M. Diamant, J.M. Dekker, M.E. Tushuizen, T. Teerlink, R.J. Heine, Alanine aminotransferase as a marker of non-alcoholic fatty liver disease in relation to type 2 diabetes mellitus and cardiovascular disease, Diabetes Metab. Res. Rev. 22 (6) (2006) 437–443, https://doi.org/10.1002/dmrr.666.
[35] A.V. Elchaninov, T.K. Fatkhudinov, P.A. Vishnyakova, A.V. Lokhonina, G.T. Sukhikh, Phenotypical and functional polymorphism of liver resident macrophages, Cells 8 (9) (2019) 1032, https://doi.org/10.3390/cells8091032.
[36] R.L. Meek, N. Eriksen, E.P. Benditt, Murine serum amyloid A3 is a high density apolipoprotein and is secreted by macrophages, Proc. Natl. Acad. Sci. USA. 89 (17) (1992) 7949–7952, https://doi.org/10.1073/pnas.89.17.7949.
[37] P. Brandtzaeg, Mucosal immunity: integration between mother and the breast-fed infant, Vaccine 21 (24) (2003) 3382–3388, https://doi.org/10.1016/S0264-410X(03)00338-4.
[38] S. Musilova, V. Rada, E. Vlkova, V. Bunesova, Beneficial effects of human milk oligosaccharides on gut microbiota, Benef. Microbes. 5 (3) (2014) 273–283, https://doi.org/10.3920/BM2013.0080.
[39] Y.G.J. Van Helden, R.W.L. Godschalk, H.J.M. Swarts, P.C.H. Hollman, F.J. Van Schooten, J. Keijer, Beta-carotene affects gene expression in lungs of male and female Bcmo1 (−/−) mice in opposite directions, Cell Mol. Life Sci. 68 (2011) 489–504, https://doi.org/10.1007/s00018-010-0461-0.
[40] I. Van der Stelt, W. Shi, M. Bekkenkamp-Grovenstein, R. Zapata-Pérez, R.H. Houtkooper, V.C.J. de Boer, et al., The female mouse is resistant to mild vitamin B3 deficiency, Eur. J. Nutr. 61 (2021) 329–340, https://doi.org/10.1007/s00394-021-02651-8.
[41] P. Portincasa, L. Bonfrate, M. Khalil, M. De Angelis, F.M. Calabrese, M. D'amato, et al., Intestinal barrier and permeability in health, obesity and NAFLD, Biomedicines 10 (1) (2022) 83, https://doi.org/10.3390/biomedicines10010083.
[42] E. Gart, E.S. Lima, F. Schuren, C.G.F. de Ruiter, J. Attema, L. Verschuren, et al., Diet-independent correlations between bacteria and dysfunction of gut, adipose tissue, and liver: a comprehensive microbiota analysis in feces and mucosa of the ileum and colon in obese mice with NAFLD, Int. J. Mol. Sci. 20 (1) (2018) 1, https://doi.org/10.3390/ijms20010001.